ChemComm

COMMUNICATION

Cite this: *Chem. Commun.*, 2018, **54**, 7022

Received 10th April 2018,
Accepted 24th May 2018

DOI: 10.1039/c8cc02855a

rsc.li/chemcomm

A live bacteria SERS platform for the *in situ* monitoring of nitric oxide release from a single MRSA†

Zhijun Zhang,[a] Xuemei Han,[a] Zhimin Wang,[a] Zhe Yang,[a] Wenmin Zhang,[ab] Juan Li,[b] Huanghao Yang,[b] Xing Yi Ling [a] and Bengang Xing *[ab]

A simple and unique surface-enhanced Raman spectroscopy (SERS) platform is developed for the precise and sensitive *in situ* monitoring of nitric oxide (NO) release from an individual bacterium. Using this live bacteria SERS platform, NO release from MRSA under the stress of antibiotics and co-infected bacteria was evaluated.

Since it was first identified as an endothelium-derived relaxation factor in 1987,[1] nitric oxide (NO) has been recognized as a ubiquitous intra- and intercellular messenger involved in diverse physiological and pathophysiological processes.[2] In mammals, NO is generated by three isoforms of NO synthase (NOS) to allow the regulation of the nervous, cardiovascular and immune systems.[3] In contrast, aberrant NO induction is closely related to several diseases such as neurodegenerative diseases, septic shock, endothelial dysfunction and cancer development.[4] Very recently, certain Gram-positive bacteria, notably *Staphylococcus* and *Bacillus* species, were discovered to encode a bacterial NO synthase (bNOS) gene similar to eukaryotic NOSs.[5] Among these NOS-producing bacterial species, methicillin-resistant *Staphylococcus aureus* (MRSA), which is a growing threat to public health as it causes increased resistance to antibiotic therapies, has drawn much attention.[6] There is increasing evidence that bNOS-derived NO plays a crucial role in MRSA antibiotic resistance, and many other diverse aspects of bacterial physiology, including bacterial virulence, oxidative stress tolerance, and biofilm formation.[7] Despite these significant achievements, the physiological functions and mechanisms of NO in bacterial physiological processes are still far from full interpretation. To better understand the roles of NO in bacterial physiology to guide the design of a bNOS targeted antibacterial strategy, methods that can precisely and sensitively probe bacterial NO are urgently demanded.

In the past few years, enormous efforts have been made to develop different advanced techniques for NO detection.[8] In particular, using fluorescence is the most promising approach for NO bioanalysis.[9] Numerous fluorescent probes have been designed for NO analysis in tissues, in living cells or even at the subcellular level.[10] These efforts have greatly promoted our understanding of NO generation in different types of cells and provided valuable insights on physiological and pathophysiological processes in a living system. However, so far, most of the studies have been mainly focused on mammalian cells, and the investigations that concentrate on the detailed understanding of bacterial NO generation have lagged far behind. In comparison to mammalian cells, bacteria are over three orders of magnitude smaller in volume, but more than ten times higher in surface to volume ratio. Hence, the drawbacks of fluorescence techniques such as the background noise from probe diffusion and autofluorescence, photobleaching and phototoxicity could be dramatically enlarged for bioanalysis in bacteria. Toward this end, to meet the demands of the precise and sensitive monitoring of NO generation in bacteria, new strategies must be developed.

Surface-enhanced Raman spectroscopy (SERS), which benefits from the localized surface plasmon resonance (LSPR) of plasmonic metal nanostructures, has emerged as a robust technique for various *in vitro* and *in vivo* bioanalytical applications.[11] The SERS technique displays many advantages for bioanalysis, including extreme sensitivity, low background, and high resolution with both spectra and imaging analysis capability.[12] SERS also offers unique advantages in resistance to photobleaching and phototoxicity over the conventional fluorescence technique.[13] These outstanding characteristics render SERS a highly competitive alternative to satisfy the demanding needs of NO biosensing. Indeed, very recently, several SERS platforms have been designed for highly sensitive and selective monitoring of NO in living mammalian cells.[14] Unfortunately, relevant NO sensing strategies suitable for bacterial bioanalysis remain under investigation, mostly due to the huge differences in the cellular structure.

Herein, we report a simple and unique plasmonic nanostructure-based live bacterial SERS platform for precise and sensitive *in situ*

[a] *Division of Chemistry and Biological Chemistry, School of Physical & Mathematical Sciences, Nanyang Technological University, Singapore, 637371, Singapore. E-mail: bengang@ntu.edu.sg*

[b] *College of Chemistry, Fuzhou University, Fuzhou, Fujian, 350116, China*

† Electronic supplementary information (ESI) available. See DOI: 10.1039/c8cc02855a

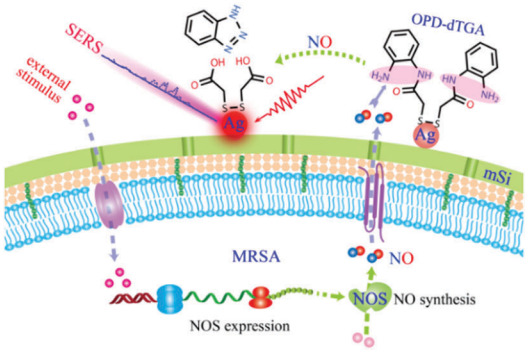

Scheme 1 Illustration of the working principle of the live bacteria SERS platform.

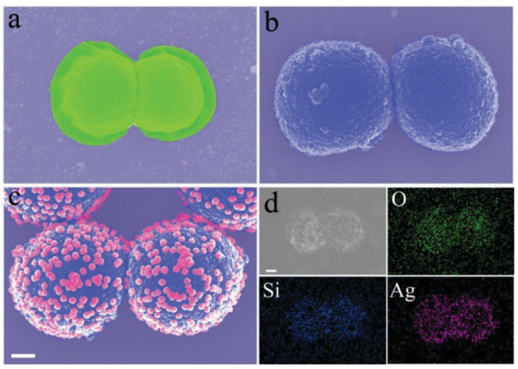

Fig. 1 False-colour SEM images of (a) bare MRSA, (b) mSi coated MRSA and (c) AgNP modified MRSA. (d) SEM image and corresponding elemental mappings of Ag, Si and O signals of the AgNP modified MRSA. Scale bar = 200 nm.

monitoring of nitric oxide release from a single bacterium. Using this platform, NO release from an MRSA strain (*e.g.* ATCC BAA-44) under the stress of different antibiotics has been fully investigated. Meanwhile, for the first time, the dose-effect relationship between antibiotics and NO generation in MRSA was analyzed. Moreover, we realized the precise SERS imaging of NO release in a polymicrobial infection model at the single-bacterium level.

The working principle of the SERS platform is schematically depicted in Scheme 1. As shown in the scheme, silver nanoparticles (AgNPs) were modified on the bacterial surface and acted as the plasmonic antenna to generate enhanced Raman signals, and a novel SERS reporter 2,2′-disulfanediylbis(*N*-(2-aminophenyl)-acetamide) (**OPD-dTGA**) that anchored on the surface of the AgNPs was designed to take charge of NO recognition. In order to achieve facile AgNP electrostatic modification and prevent bacterial activity perturbation induced by direct contact with the AgNPs, prior to AgNP modification, bacteria biomineralization was first carried out with a thin amino-functionalized mesoporous silica (mSi) layer through our method reported previously.[15] Typically, two functional groups are involved in such a well-defined SERS probe. Firstly, the disulfide group was rationally designed for anchoring the probe onto the surface of the AgNPs through the stable Ag–S bond. Secondly, the *o*-phenylenediamine group, a highly selective and efficient NO-responsive motif,[16] was conjugated for NO recognition and SERS signal generation. Specifically, NO generated from MRSA upon external stimulation could cleave the SERS probe to form free benzotriazole and carboxyl groups, which thus leads to a strong SERS variation for effective bio-sensing.

The SERS sensing platform was first fabricated and characterized using various techniques. As a proof of concept, the MRSA strain (ATCC BAA-44) was used as a model bacterium. The SEM imaging and element mapping results indicated the successful fabrication of the plasmonic platform (Fig. 1). Typically, bare MRSA was found to be shrivelled during drying (Fig. 1a). After coating with a silica layer, a nearly spherical shape with a smooth surface was formed (Fig. 1b). Through electrostatic interaction, more than two hundred AgNPs were found to be decorated on each MRSA (Fig. 1c and d). Such high density and uniform modification would help to generate a strong and homogeneous SERS signal for effective bioanalysis. The TEM image, UV-vis spectra and zeta potential analysis further confirmed the successful fabrication of the SERS platform (Fig. S1–S4, ESI†). The silica layer was found to be uniformly encapsulated around the bacteria with a thickness of ~50 nm (Fig. S2, ESI†). The pore diameter of the mSi was about 7 nm from the N_2 absorption–desorption isotherms (Fig. S5, ESI†), which will facilitate fast mass transportation. Based on the elemental composition from the ICP-OES analysis, the molar ratio between the probe and the silver nanoparticle was further estimated to be over ten thousand. Considering the *in situ* monitoring of NO generation in live bacteria, the effect of the AgNPs and probe immobilization on MRSA viability was then investigated. Through live/dead staining with standard indicators, fluorescein diacetate (FDA) – propidium iodide (PI), the surface modified MRSA was demonstrated to retain a high validity with over 90% of the survival rate (Fig. S6, ESI†). This signified that the modification of the AgNPs and the probe would cause minimal perturbation on the bioactivity of the bacteria (Fig. S7, ESI†). Besides, the growth curves further revealed that the modified MRSA remained in an unamplified status for at least 14 h (Fig. S8, ESI†), which provides the feasibility to collect a reliable and stable SERS signal for effective detection.

The reactivity of the probe towards NO was then verified through HPLC analysis. The probe exhibited a single pure peak around 5 min (in magenta color) in the HPLC profile (Fig. 2a). In the presence of NO, a decrease in the peak area, together with a new peak around 3.5 min (in cyan color), was observed, ascribed to the product formation of benzotriazole (Fig. S9, ESI†). The increased NO could lead to a further decrease in the probe peak and a corresponding area increase in the benzotriazole peak, revealing that the probe could be cleaved in a NO concentration-dependent manner.

Furthermore, the SERS spectra of the probe in the absence and presence of NO were measured. As shown in Fig. 2b, the probe possessed abundant intense SERS signals. The main peaks at 1233, 1263, 1322 and 1349 cm^{-1} were attributed to the amide III modes. The strongest peak at 1446 cm^{-1} could be assigned to aromatic C–C stretching modes. Meanwhile, a distinct band around 960 cm^{-1} assigned to multi-phonon scattering generated in the Si substrate could be observed. Incubating the probe with NO will lead to an apparent decrease

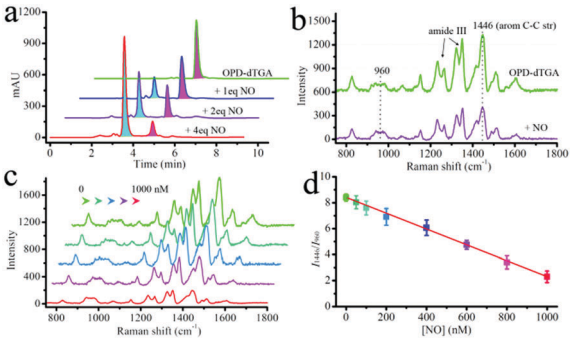

Fig. 2 (a) HPLC analysis of the probe upon reaction with NO. The probe peak was in magenta, and the peak of benzotriazole was in cyan. (b) SERS spectra of the probe with or without NO. (c) The SERS spectra of the probe under different concentrations of NO (0, 50, 200, 600, and 1000 nM). (d) The plot of I_{1446}/I_{960} as a function of NO concentration.

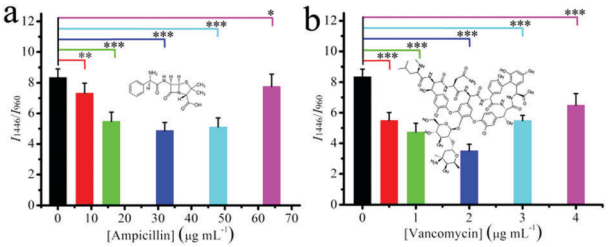

Fig. 3 SERS signal changes in the MRSA after exposure with different concentrations of (a) ampicillin and (b) vancomycin. Significant difference: $^{*}P < 0.05$, $^{**}P < 0.01$, $^{***}P < 0.001$.

in all the characteristic peaks from the probe. The cleavage of the aromatic group in the NO reporter was considered to be responsible for the attenuation since there was no detectable SERS signal from the dithiodiglycolic acid (Fig. S10, ESI†), which was the residual group of the reporter upon NO treatment.[16] Remarkably, after NO treatment, there was almost no change for the band around 960 cm^{-1}, which could act as a reference for the ratiometric analysis. The optimal condition for probe immobilization was also studied. The strongest signal could be observed after incubation with 1 mM of the probe for 30 min (Fig. S11, ESI†). Moreover, it was found that the SERS signal could reach saturation within 30 min (Fig. S12, ESI†), suggesting a fast response to NO in the sensing process.

We further examined the SERS signal variation under spiking with a series of concentrations of NO (Fig. 2c). As expected, the peak intensity of the probe decreased gradually with the increasing NO concentration. A linear relationship between the ratiometric intensity of I_{1446}/I_{960} and the concentration of NO was identified with the detection limit (triple signal-to-noise ratio) less than 100 nM (Fig. 2d). The SERS response to other different ROS was subsequently investigated. NO could trigger a significant SERS intensity change (Fig. S13, ESI†). In contrast, other ROS (*e.g.* $ONOO^-$, ClO^-, H_2O_2, $^{\bullet}OH$, $^1O_2$, and O_2^- *etc.*) could not induce apparent changes in the SERS signal even at high concentration, clearly indicating the high selectivity of the probe toward NO. Moreover, the platform demonstrated impressive long-term stability, as the SERS signal remained almost unchanged even after one-week of storage (Fig. S14, ESI†).

Consequently, the feasibility of the *in situ* detection of bacterial NO under the stress of antibiotic treatment was further investigated. Generally, bNOS-derived NO generation is closely related to antibiotic resistance in MRSA, in which NO was produced to engage in MRSA self-protection.[7a] To explore the dose-effect relationship between antibiotics and NO generation in MRSA, we examined the NO release from MRSA under the stress of different antibiotics with a series of concentrations. As a proof of concept, we chose ampicillin (a commonly used penicillin beta-lactam antibiotic), and vancomycin (a glycopeptide antibiotic as last resort against MRSA) as the two representative drug molecules.[17]

As presented in Fig. 3, both the antibiotics could stimulate significant NO generation in MRSA. The NO produced by the MRSA ranges from 100–600 nM upon ampicillin stimulation, and 300–800 nM for vancomycin (Fig. S15, ESI†). At the low concentration, NO production was enhanced upon increasing the antibiotics, while the further increased antibiotics led to a decrease in NO generation. The inflection points were found to be around the MICs of the antibiotics (*e.g.* ampicillin: ~32 μg ml^{-1} and vancomycin: ~2 μg ml^{-1}).[17,18] This phenomenon is considered to be related to the impact of antibiotics on bacterial activity. In comparison, vancomycin triggered more NO production in MRSA than ampicillin. Such differences were mostly caused by the different susceptibilities of MRSA against the two antibiotics, as MRSA is known to be resistant to ampicillin but susceptible to vancomycin.[18] When in the presence of a NOS inhibitor *N*ω-nitro-L-arginine methyl ester hydrochloride (L-NAME), the antibiotic induced NO production was greatly suppressed (Fig. S16, ESI†), which demonstrated that antibiotic induced upregulation of NOS expression was responsible for the NO generation. Notably, in the absence of antibiotics, the inhibitor did not cause any noticeable difference in the SERS signal, revealing that there was almost no detectable amount of NO released from MRSA in the tested conditions without stimulation. As the control, the NO synthesis was also measured in a Gram-negative strain *Escherichia coli* K-12 without the bNOS gene (Fig. S17 and S18, ESI†). As expected, there was no evident NO generation in K-12 upon antibiotic treatment, indicating very different NO generation from the MRSA.

Finally, the capacity of this SERS platform to give a direct imaging view of NO generation in a model of polymicrobial infection was also examined. In clinical settings, MRSA suffering patients are often co-infected with other pathogens such as *Pseudomonas aeruginosa*, one of the frequently reported species to cause clinical infections.[19] Under polymicrobial stimulation, the NOSs would be overexpressed in MRSA to improve their survivability.[7c,19] Hence, to this end, we built a polymicrobial infection model by the co-culture of the modified MRSA with *Pseudomonas aeruginosa* (PA01) for the direct view of NO production. As shown in Fig. 4, the clear SERS imaging of the single-bacterium was observed by monitoring the signal change at 1446 cm^{-1} (Fig. 4). Typically, the MRSA alone showed a high imaging signal from the NO reporter (Fig. 4, left). However, after co-culture with PA01, the imaging signal was found to be sharply reduced (Fig. 4, middle), suggesting that the co-cultured PA01 could trigger NO synthesis in MRSA. The pyocyanin secreted

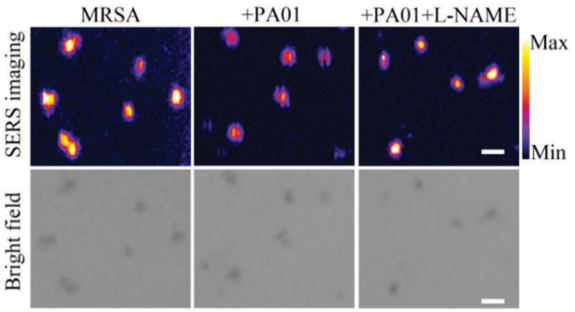

Fig. 4 SERS images monitored at 1446 cm^{-1} of the MRSA after being cultured in LB (the left), co-cultured with PA01 (the middle) and co-cultured in the presence of the NOS inhibitor (the right). The pictures in the bottom row show their corresponding bright field images. Scale bar = 2 μm.

from PA01 was considered to be responsible for the stimulation of NO synthesis in MRSA,[7c] which was further confirmed by monitoring the UV-vis absorbance of the medium (Fig. S19, ESI†). As a control, a co-culture group with the NOS inhibitor (L-NAME) was investigated. Apparently, in the presence of L-NAME, an enhanced imaging signal was observed (Fig. 4, right), indicating that the upregulation of NOS expression was responsible for PA01 induced NO synthesis in MRSA.

In summary, we presented a simple and unique plasmonic nanostructure-based live bacteria SERS platform for the precise and sensitive *in situ* monitoring of nitric oxide release from an individual bacterium. The SERS platform was fabricated by the combination of a novel NO reporter with a plasmonic nanostructure, which was demonstrated to be highly selective, sensitive and fast responsive towards NO generation. Using this platform, we elucidated that both the antibiotics ampicillin and vancomycin could induce NO generation in MRSA in a concentration-dependent manner. Moreover, we realized the *in situ* and precise SERS imaging of NO release at a single MRSA level in a polymicrobial infection model. This work not only provides more understanding of NO generation in bacterial physiological processes but also affords a new idea to fabricate a SERS platform for the sensing of various bacteria secretions.

This work was partially supported by NTU-AIT-MUV NAM/16001, RG110/16 (S), (RG11/13) and (RG35/15), NTU-JSPS JRP grant (M4082175.110) awarded in the Nanyang Technological University, Singapore and the National Natural Science Foundation of China (NSFC) (No. 51628201).

Conflicts of interest

There are no conflicts to declare.

References

1 L. J. Ignarro, G. M. Buga, K. S. Wood, R. E. Byrns and G. Chaudhuri, *Proc. Natl. Acad. Sci. U. S. A.*, 1987, **84**, 9265.
2 (*a*) C. Bogdan, *Trends Immunol.*, 2015, **36**, 161; (*b*) D. Fukumura, S. Kashiwagi and R. K. Jain, *Nat. Rev. Cancer*, 2006, **6**, 521.
3 U. Förstermann and W. C. Sessa, *Eur. Heart J.*, 2012, **33**, 829.
4 A. Pautz, J. Art, S. Hahn, S. Nowag, C. Voss and H. Kleinert, *Nitric oxide*, 2010, **23**, 75.
5 T. L. Kinkel, S. Ramos-Montañez, J. M. Pando, D. V. Tadeo, E. N. Strom, S. J. Libby and F. C. Fang, *Nat. Microbiol.*, 2016, **2**, 16224.
6 (*a*) Q. Shao, Y. Zheng, X. Dong, K. Tang, X. Yan and B. G. Xing, *Chem. – Eur. J.*, 2013, **19**, 10903; (*b*) Q. Shao and B. G. Xing, *Chem. Commun.*, 2012, **48**, 1739; (*c*) W. Li, K. Dong, J. Ren and X. Qu, *Angew. Chem., Int. Ed.*, 2016, **55**, 8049.
7 (*a*) N. M. van Sorge, F. C. Beasley, I. Gusarov, D. J. Gonzalez, M. von Köckritz-Blickwede, S. Anik, A. W. Borkowski, P. C. Dorrestein, E. Nudler and V. Nizet, *J. Biol. Chem.*, 2013, **288**, 6417; (*b*) D. P. Arora, S. Hossain, Y. Xu and E. M. Boon, *Biochemistry*, 2015, **54**, 3717; (*c*) I. Gusarov, K. Shatalin, M. Starodubtseva and E. Nudler, *Science*, 2009, **325**, 1380.
8 (*a*) J. H. Kim, D. A. Heller, H. Jin, P. W. Barone, C. Song, J. Zhang, L. J. Trudel, G. N. Wogan, S. R. Tannenbaum and M. S. Strano, *Nat. Chem.*, 2009, **1**, 473; (*b*) E. Eroglu, B. Gottschalk, S. Charoensin, S. Blass, H. Bischof, R. Rost, C. T. Madreiter-Sokolowski, B. Pelzmann, E. Bernhart, W. Sattler, S. Hallström, T. Malinski, M. Waldeck-Weiermair, W. F. Graier and R. Malli, *Nat. Commun.*, 2016, **7**, 10623.
9 (*a*) Y. Q. Sun, J. Liu, H. Zhang, Y. Huo, X. Lv, Y. Shi and W. Guo, *J. Am. Chem. Soc.*, 2014, **136**, 12520; (*b*) J. Wang, C. He, P. Wu, J. Wang and C. Duan, *J. Am. Chem. Soc.*, 2011, **133**, 12402; (*c*) H. Yu, Y. Xiao and L. Jin, *J. Am. Chem. Soc.*, 2012, **134**, 17486; (*d*) L. Yuan, W. Lin, Y. Xie, B. Chen and S. Zhu, *J. Am. Chem. Soc.*, 2012, **134**, 1305.
10 (*a*) X. Chen, L. Sun, Y. Chen, X. Cheng, W. Wu, L. Ji and H. Chao, *Biomaterials*, 2015, **58**, 72; (*b*) X. Liu, S. Liu and G. Liang, *Analyst*, 2016, **141**, 2600; (*c*) H. W. Yao, X. Y. Zhu, X. F. Guo and H. Wang, *Anal. Chem.*, 2016, **88**, 9014; (*d*) Z. Dai, L. Tian, B. Song, X. Liu and J. Yuan, *Chem. Sci.*, 2017, **8**, 1969; (*e*) Z. Mao, W. Feng, Z. Li, L. Zeng, W. Lv and Z. Liu, *Chem. Sci.*, 2016, **7**, 5230; (*f*) N. Wang, X. Yu, K. Zhang, C. A. Mirkin and J. Li, *J. Am. Chem. Soc.*, 2017, **139**, 12354.
11 (*a*) L. J. Xu, Z. C. Lei, J. Li, C. Zong, C. J. Yang and B. Ren, *J. Am. Chem. Soc.*, 2015, **137**, 5149; (*b*) S. R. Panikkanvalappil, M. James, S. M. Hira, J. Mobley, T. Jilling, N. Ambalavanan and M. A. El-Sayed, *J. Am. Chem. Soc.*, 2016, **138**, 3779; (*c*) Q. Jin, M. Li, B. Polat, S. K. Paidi, A. Dai, A. Zhang, J. V. Pagaduan, I. Barman and D. H. Gracias, *Angew. Chem., Int. Ed.*, 2017, **56**, 3822; (*d*) S. Tanwar, K. K. Haldar and T. Sen, *J. Am. Chem. Soc.*, 2017, **139**, 17639; (*e*) L. Xu, S. Zhao, W. Ma, X. Wu, S. Li, H. Kuang, L. Wang and C. Xu, *Adv. Funct. Mater.*, 2016, **26**, 1602; (*f*) J. Morla-Folch, P. Gisbert-Quilis, M. Masetti, E. Garcia-Rico, R. A. Alvarez-Puebla and L. Guerrini, *Angew. Chem., Int. Ed.*, 2017, **56**, 2381.
12 (*a*) A. Kumar, S. Kim and J. M. Nam, *J. Am. Chem. Soc.*, 2016, **138**, 14509; (*b*) D. Cialla-May, X. S. Zheng, K. Weber and J. Popp, *Chem. Soc. Rev.*, 2017, **46**, 3945; (*c*) L. E. Jamieson, S. M. Asiala, K. Gracie, K. Faulds and D. Graham, *Annu. Rev. Anal. Chem.*, 2017, **10**, 415; (*d*) J. Zhang, P. Joshi, Y. Zhou, R. Ding and P. Zhang, *Chem. Commun.*, 2015, **51**, 15284; (*e*) X. Kuang, S. Ye, X. Li, Y. Ma, C. Zhang and B. Tang, *Chem. Commun.*, 2016, **52**, 5432; (*f*) M. S. Strozyk, D. J. de Aberasturi, J. V. Gregory, M. Brust, J. Lahann and L. M. Liz-Marzán, *Adv. Funct. Mater.*, 2017, **27**, 1701626.
13 D. W. Li, L. L. Qu, K. Hu, Y. T. Long and H. Tian, *Angew. Chem., Int. Ed.*, 2015, **54**, 12758.
14 (*a*) P. Rivera_Gil, C. Vazquez-Vazquez, V. Giannini, M. P. Callao, W. J. Parak, M. A. Correa-Duarte and R. A. Alvarez-Puebla, *Angew. Chem., Int. Ed.*, 2013, **52**, 13694; (*b*) J. Cui, K. Hu, J. J. Sun, L. L. Qu and D. W. Li, *Biosens. Bioelectron.*, 2016, **85**, 324; (*c*) Q. Xu, W. Liu, L. Li, F. Zhou, J. Zhou and Y. Tian, *Chem. Commun.*, 2017, **53**, 1880.
15 Z. Zhang, E. Ju, W. Bing, Z. Wang, J. Ren and X. Qu, *Chem. Commun.*, 2017, **53**, 8415.
16 H. Zheng, G. Q. Shang, S. Y. Yang, X. Gao and J. G. Xu, *Org. Lett.*, 2008, **10**, 2357.
17 B. G. Xing, C. W. Yu, P. L. Ho, K. H. Chow, T. Cheung, H. Gu, Z. Cai and B. Xu, *J. Med. Chem.*, 2003, **46**, 4904.
18 T. Gverzdys, M. K. Hart, S. Pimentel-Elardo, G. Tranmer and J. R. Nodwell, *J. Antibiot.*, 2015, **68**, 698.
19 N. Nair, R. Biswas, F. Götz and L. Biswas, *Infect. Immun.*, 2014, **82**, 2162.